Generative model-based underwater acoustic channel modeling with partial oceanic environmental parameters

Hongbo Miao
National Key Laboratory of Underwater Acoustic Technology, Harbin Engineering University
Key Laboratory for Polar Acoustics and Application of Ministry of Education
College of Underwater Acoustic Engineering, Harbin Engineering University
Harbin , China
urbino_hb_miao@hrbeu.edu.cn

Li Li
National Key Laboratory of Underwater Acoustic Technology, Harbin Engineering University
Key Laboratory for Polar Acoustics and Application of Ministry of Education
College of Underwater Acoustic Engineering, Harbin Engineering University
Harbin , China
li.li@hrbeu.edu.cn

Manxin Liu
National Key Laboratory of Underwater Acoustic Technology, Harbin Engineering University
Key Laboratory for Polar Acoustics and Application of Ministry of Education
College of Underwater Acoustic Engineering, Harbin Engineering University
Harbin , China
liumanxin@hrbeu.edu.cn

Hui Sun
College of Underwater Acoustic Engineering, Harbin Engineering University
Harbin , China
heusunhui@126.com

2024 IEEE International Conference on Signal Processing, Communications and Computing (ICSPCC) | 979-8-3503-6655-6/24/$31.00 ©2024 IEEE | DOI: 10.1109/ICSPCC62635.2024.10770456

***Abstract*—In this paper, a generative model-based underwater acoustic (UWA) channel modeling method with partial oceanic environmental parameters is proposed. This method integrates the outputs produced by conventional channel models as priors to solving the dilemma posed by traditional UWA channel modeling tasks: difficulties obtaining comprehensive parameters from experimental observations due to the poor understanding of detailed underlying physics. Generative adversarial networks (GANs) capture the distribution of UWA signals received within a period. Well-trained GANs can generate channel impulse responses (CIRs) that resemble real CIRs. The experimental results, supported by field data acquired from shallow water environments, indicate that the proposed method is able to model UWA channels and possesses the ability to generalize to small-scale temporal variations within a period. Specifically, the deep convolutional Wasserstein generative adversarial network with a gradient penalty (DCWGAN-GP) significantly improves upon the performance of the traditional channel model, and the mean absolute error (MAE) of the CIRs is enhanced by 57.3 % under a SNR=10 dB.**

Keywords—generative model; underwater acoustic channel; channel modeling; physics model integration.

I. INTRODUCTION

UWA channels are commonly regarded as challenging wireless communication media in which transmitted signals exhibit various characteristics, e.g., attenuation, delays, and multipath effects, due to the reflection, refraction, and scattering of acoustic waves[1], [2]. To address the inherent complexity of UWA channels, it is essential to study the characteristics of such channels systematically. The investigation of the statistical characteristics of UWA channels serves as a cornerstone for developing robust, efficient, and adaptable communication systems in the face of limited temporal or spatial UWA resources [3]. Therefore, pursuing a UWA channel model that possesses reusability, validity, and generalization ability is paramount. In previous works, UWA channel characteristics were investigated using both modeling methods and experimental measurement methods[4], [5], [6]. Channel modeling aims to extract the physical processes governing sound propagation in underwater environments and to encapsulate effects such as multipath scattering, temperature and salinity gradients, and sea surface and seafloor reflections. Experimental methods, including channel sounding and field measurements, offer empirical data crucial for validating and refining these models. UWA physical-based channel modeling methods can be divided into two categories: deterministic models[7] and statistical models[8], [9]. Deterministic models include ray-tracing models, wave equation models, and finite element models. Statistical models include empirical models and stochastic models. In addition, UWA channels have been represented as mathematical models[10], and simulation models[11]. Developing tractable mathematical descriptions for UWA channels is challenging due to the complex interaction of environmental parameters on sound propagation, including reflection, refraction, scattering, and reverberation, as well as the presence of marine life and other factors. As a result, traditional channel models resort to simplifications and assumptions and may not fully involve comprehensive oceanic environmental parameters. Moreover, estimating the parameters of conventional UWA channel models from experimental observations is particularly difficult, given the incomplete understanding of the intricate underlying physical processes. Aiming to address these problems, this paper utilizes the capabilities of deep generative models to capture other implicit oceanic environmental parameters inherent in received UWA signals and refine the precision of conventional channel models.

The capability of GANs suggests that proficiently trained GANs can potentially generate synthesized signals that closely match the distribution of real signals. Intuitively, by exploiting the generator (G) of such a trained GAN, abundant synthesized signals that nearly conform to the distribution of the real signals can be obtained. Using the orthogonal matching pursuit (OMP) technique, the channel delay and amplitude are extracted from the synthesized UWA signals.

In our study, coarse modeling results are produced by a traditional channel model BELLHOP, which can rapidly simulate the UWA channel based on the range and depth of the transmitter and receiver, ocean sound speed profile (SSP), and other oceanic environment parameters. This method contrasts with the vanilla GAN, which uses a random vector to model real signals, as this random vector contains no helpful information to aid in generating synthesized signals. In this manner, a well-trained G can refine the outputs of the BELLHOP model by integrating actual received UWA signals embedded with authentic oceanic environmental information, yielding a more precise model.

In response to the challenging and unstable task of training GANs, which includes convergence difficulties, modal collapse, and vanishing gradient [12], this study explores two aspects of GANs. On the one hand, we refine the loss function of our GAN by incorporating a regularization term into the signal amplitude learning process. On the other hand, to better capture the statistical inform-ation and distribution characteristics of received signals, a convolutional neural network (CNN) is introduced as the structure for both G and discriminator (D). Moreover, to improve convergence, the two-time-scale update rule (TTUR)[13] is employed, replacing the traditional approach wherein identical learning rates and update rules are applied to both G and D. Furthermore, the MAE performance of these generative models integrating the outputs of BELLHOP is analyzed, namely, DCWGAN-GP^{B}, DCWGAN^{B}, and DCGAN^{B}. According to the experimental results, DCWGAN-GP^{B} performed best overall.

II. SYSTEM MODEL

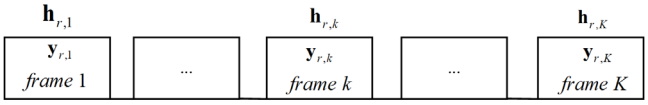

Fig. 1. The structure of the received signals.

In this paper, the discretely sampled transmitted signal $\mathbf{x}_t(n)=[x_t(1),...,x_t(Q)]^T \in \mathbb{R}^Q$ is transmitted at a regular interval, as shown in Fig. 1 (we consider that over a short period of time, a UWA channel can be approximated as a small-scale channel[3]). The received signals $\mathbf{y}_{r,k}(n)=[y_{r,k}(1),...,y_{r,k}(N)]^T \in \mathbb{R}^N$, for the k th frame can be denoted as

$$\mathbf{y}_{r,k}(n)=\mathbf{x}_t(n)*\mathbf{h}_{r,k}(n)+\mathbf{w}_k(n) \tag{1}$$

where $\mathbf{w}_k(n)=[w_k(1),...,w_k(N)]^T \in \mathbb{R}^N$ is additive white Gaussian noise that conforms to a Gaussian distribution of $\mathbf{w}_k(n) \sim \mathcal{N}(0,\sigma_w^2)$, * denotes linear convolution and the CIR $\mathbf{h}_{r,k}(n)=[h_{r,k}(1),...,h_{r,k}(P)]^T \in \mathbb{R}^P$ of the k th frame is commonly represented as

$$\mathbf{h}_{r,k}(n)=\sum_{i=0}^{r-1} A_i \delta(n-\tau_i) \tag{2}$$

where is the number of multipath, δ is the impulse response function; and A_i and τ_i are the amplitude and time delay of the multipath, respectively.

In this paper, due to the sparsity of UWA channels, an extensively used theoretical compressive sensing approach, the OMP estimation method[14], is exploited in the proposed GAN-based algorithm. In our study, according to various channel structures, the sparsity of OMP is set to an appropriate value to obtain a relatively accurate CIR.

III. GENERATIVE MODEL-BASED UWA CHANNEL MODELING

A. Modified DCWGAN-GP Model

The WGAN replaces the Jensen-Shannon divergence (JSD) with the Wasserstein distance, which can be described as the cost of transforming one data distribution into another. More precisely, this approach quantifies the similarity between two probability distributions; in our study, one distribution is the synthesized signal distribution p_f, and the other is the real signal distribution p_r. The Wasserstein distance between two probability distributions can be expressed as

$$W(p_r,p_f)=\inf_{\gamma\in\Pi(p_r,p_f)} \mathbb{E}_{(\mathbf{x},\mathbf{y})\sim\gamma}[\|\mathbf{x}-\mathbf{y}\|] \tag{3}$$

which can be seen as a lower bound (infimum) for transitioning between $\mathbf{x}$ and $\mathbf{y}$, where $\Pi(p_r,p_f)$ denotes the collection of all joint probability distributions $\gamma(\mathbf{x},\mathbf{y})$ th-at possess p_r and p_f as their respective marginal distri-butions and $\|\cdot\|$ is a distance metric, such as the Euclidean distance. However for (3), it is difficult to achieve minimi-zation unless its dual form is used according to the Kantorovich-Rubinstein duality theorem[15]. The dual form of the Wasserstein distance is

$$\begin{aligned} W(p_r,p_f)=\frac{1}{K}\sup_{\|f\|_L\le K}\Big[&\mathbb{E}_{\mathbf{y}_{r,k}\sim p_r(\mathbf{y}_{r,k})}[f(\mathbf{y}_{r,k})]- \\ &\mathbb{E}_{\mathbf{y}_{f,k}\sim p_f(\mathbf{y}_{f,k})}[f(\mathbf{y}_{f,k}))]\Big] \\ \text{s.t. } &|f(x_1)-f(x_2)|\le K|x_1-x_2| \end{aligned} \tag{4}$$

where f is a K-Lipschitz function following the constraint in (4) and sup represents the supremum, which is the least upper bound among all the elements in a set. According to the universal approximation theorem of neural networks[16], we assume that there is a neural network $f(x;\phi)$ (a CNN is used in our study) that can maximize (4), assuming that a parameter set Φ exists; for all $\phi\in\Phi$, $f(x;\phi)$ is a K-Lipschitz continuous function. In this paper, $K=1$. Thus far, the calculation of the minimum value problem of the original W-distance has been transformed into a problem of seeking the maximum value in this dual form. (4) can be approximated as

$$\max_{\phi\in\Phi}\Big[\mathbb{E}_{\mathbf{y}_{r,k}\sim p_r(\mathbf{y}_{r,k})}[f(\mathbf{y}_{r,k};\phi)]-\mathbb{E}_{\mathbf{y}_{f,k}\sim p_f(\mathbf{y}_{f,k})}[f(\mathbf{y}_{f,k};\phi)]\Big] \tag{5}$$

To enforce the Lipschitz constraint from (4), Arjovsky proposed weight clipping, where the weights of D are clipped to a small range. However, this approach can lead to optimization difficulties and affect the quality of the gener-ated signals[15]. Alternatives such as the gradient penalty have been proposed to alleviate these issues. The gradient penalty is

$$GP(D)=\mathbb{E}_{\hat{\mathbf{y}}\sim p_{sample}(\hat{\mathbf{y}})}\left[\left(\left\|\nabla_{\hat{\mathbf{y}}}D(\hat{\mathbf{y}};\theta_d)\right\|_2-1\right)^2\right] \tag{6}$$

where $\hat{\mathbf{y}}$ is derived by summing two components; the first is the product of a random number α drawn from a uniform distribution $\mathcal{U}(0,1)$ and an actual signal $\mathbf{y}_{r,k}$, and the second is the product of the complement of $1-\alpha$ and a synthesized signal $\mathbf{y}_{f,k}$. The process for sampling $\hat{\mathbf{y}}$ is depicted in the block diagram on the seafloor on the right side of . By including the gradient penalty term, the loss function for D is

$$\begin{aligned} \mathcal{L}_D=&\mathbb{E}_{\mathbf{y}_{r,k}\sim p_{r,k}(\mathbf{y}_{r,k})}[D(\mathbf{y}_{r,k};\theta_d)]- \\ &\mathbb{E}_{\mathbf{y}_{b,k}\sim p_b(\mathbf{y}_{b,k})}[D(G(\mathbf{y}_{b,k};\theta_g);\theta_d)]-\lambda GP(D) \end{aligned} \tag{7}$$

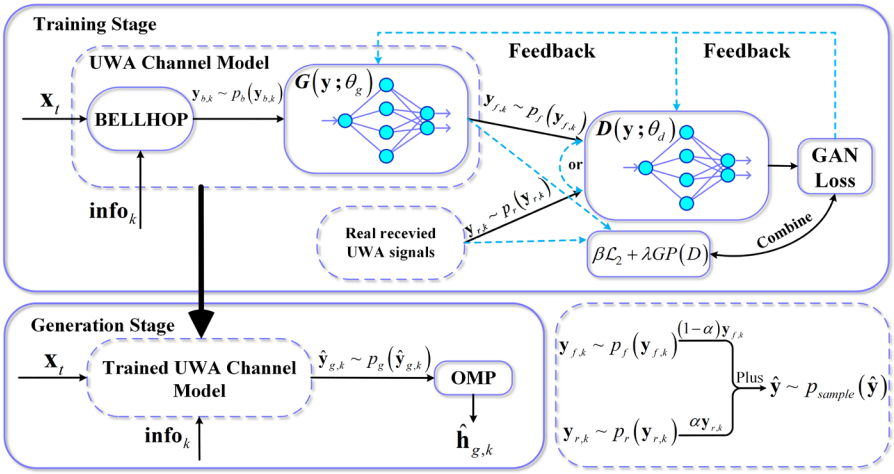

Fig. 2. Diagram of the proposed overall framework with its inputs and outputs.

where λ is a hyperparameter that controls the strength of the penalty term. Moreover, to ensure that the signal amplitude is learned by G in the correct direction, we incorporate a 2-norm regularization loss into G. The loss function of G is represented as follows:

$$\mathcal{L}_G = -\mathbb{E}_{\mathbf{y}_{b,k}\sim p_{b,k}(\mathbf{y}_{b,k})}\left[D(G(\mathbf{y}_{b,k};\theta_g);\theta_d)\right] + \beta\mathcal{L}_2 \quad (8)$$

where $\mathcal{L}_2(\mathbf{y}_{r,k},\mathbf{y}_{f,k}) = \mathbb{E}\left[\|\mathbf{y}_{r,k}-\mathbf{y}_{f,k}\|_2\right]$ and β is the regularization coefficient. Therefore, the total loss function of the DCWGAN-GP is

$$\begin{aligned}\mathcal{L}_{DCWGAN-GP} = {} & \mathbb{E}_{\mathbf{y}_{r,k}\sim p_r(\mathbf{y}_{r,k})}\left[D(\mathbf{y}_{r,k};\theta_d)\right] - \\ & \mathbb{E}_{\mathbf{y}_{b,k}\sim p_b(\mathbf{y}_{b,k})}\left[D(G(\mathbf{y}_{b,k};\theta_g);\theta_d)\right] - \lambda GP(D) + \beta\mathcal{L}_2\end{aligned} \quad (9)$$

B. Generative Model-Based UWA Channel Modeling

The generative model-based algorithm for UWA channel modeling proposed in this study consists of two phases, an adversarial training stage and a generation stage, both of which are illustrated in Fig. 2. To ensure that the distribution $p_{f,k}$ of the generated (synthesized) received signals produced by G is close to the real received signal distribution characterized by $p_r(\mathbf{y}_{r,k})$, we utilize the modified DCWGAN-GP framework to conduct the adversarial training stage. Throughout this adversarial phase, the framework is designed to approximate the true signal distribution described by $p_r(\mathbf{y}_{r,k})$. A well-trained UWA channel model is considered a real ocean channel that contains various experimental information from a fixed ocean area. Afterward, in the generation stage, given the transmitted signals $\mathbf{x}_t$, and random oceanic environmental information (e.g., SSP), the signal modeling process is implemented by generating the synthesized received signals. Utilizing these newly synthesized signals, channel information can be performed through the application of the OMP estimation method. In Fig. 2, we detail the steps of the proposed generative model-based algorithm, which begins with the adversarial training stage.

(1) *Adversarial Training Stage*: The received signal $\mathbf{y}_{r,k}$ for the k th frame, $k\in[1,300]$ is used as the real training data (i.e., $\mathbf{y}_{r,k}\sim p_r(\mathbf{y}_{r,k})$) for adversarially training the DCWGAN-GP. Furthermore, $\mathbf{y}_{b,k} = \text{BELLHOP}(\mathbf{info}_k)*\mathbf{x}_t$, where BELLHOP(·) operates on the given experimental information $\mathbf{info}_k = \left[\mathbf{ssp}_k^T, \mathbf{env}^T\right]^T$ of the k th frame, $k\in[1,300]$ and outputs CIR $\mathbf{h}_{b,k}$ of the k th frame, $k\in[1,300]$, $\mathbf{y}_{b,k}$ is referred to as the BELLHOP signal. Owing to the impracticality of conducting SSP measurements for each individual frame during actual sea trials, particularly in situations characterized by short signal transmission durations, we utilize a method whereby minor perturbation are introduced to measured ssp_{ori}, a one-dimensional vector that denotes the variation exhibited by the sound speed with increasing ocean depth. This process is applied for each frame, with the objective of approximating the real SSP corresponding to that frame. Subsequently, $\mathbf{y}_{b,k}\sim p_b(\mathbf{y}_{b,k})$, which is obtained by BELLHOP through coarse modeling, is fed into G. Intuitively, in contrast to G's conventional practice of sampling noise from Gaussian or other distributions, G can leverage $\mathbf{y}_{b,k}$ as a form of prior knowledge.

(2) *UWA Channel Generation Stage*: As shown in Fig. 2, by using $\mathbf{x}_t$, test environmental information $\mathbf{info}_k$, $k\in(300,400]$ as the inputs, channel modeling is implemented 100 times in the generation stage. The k th synthesized signal is obtained through $\mathbf{y}_{b,k} = \text{BELLHOP}(\mathbf{info}_k)*\mathbf{x}_t$. Note that $\hat{\mathbf{y}}_{g,k}\in\mathbb{R}^N$, i.e., $\hat{\mathbf{y}}_{g,k}$ and $\mathbf{y}_{r,k}$ are vectors with the same length. Moreover, $\hat{\mathbf{y}}_{g,k}$ nearly conforms to the distribution $p_r(\mathbf{y}_{r,k})$, $k\in(300,400]$. Therefore, the CIR $\hat{\mathbf{h}}_{g,k}$ can be estimated by conducting OMP with $\mathbf{x}_t$ and $\hat{\mathbf{y}}_{g,k}$. The algorithm in question is sequentially executed within each transmission frame.

From Fig. 3, under identical numbers of training iterations, the convergence curves of both DCWGAN-GP and DCWGAN-GP$^{\text{B}}$ fluctuate significantly during the initial 300 iterations, after which the GAN loss function oscillates around 0. However, DCWGAN-GP exhibits more significant fluctuations after 500 iterations than DCWGAN-GP$^{\text{B}}$. This indicates that integrating the modeling results of BELLHOP can effectively improve the convergence and stability of the model. Therefore, BELLHOP signals are used in this study

to enhance the training stability of models. This decision is based on the fact that BELLHOP-simulated signals can provide G with an initial distribution, which is more effective than feeding G random noise.

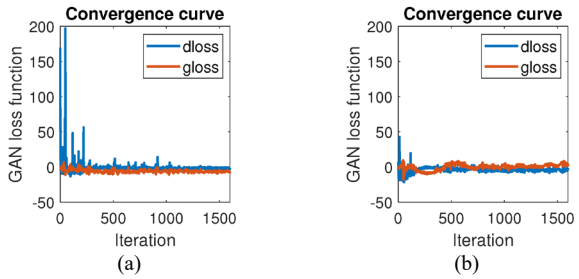

Fig. 3. Convergence curves produced under an SNR of 10 dB, red line is $\mathcal{L}_G$, blue line is $\mathcal{L}_D$. (a) DCWGAN-GP^{B}. (b) DCWGAN-GP.

C. Network architecture and parameters setting

The G of each GAN starts with a 128-dimensional input dense layer, followed by a series of upsampling blocks (ups-blocks). An ups-block is composed of an upsampling layer that extends the dimensionality to double the original size, a one-dimensional convolutional layer and an instance normalization layer that is able to accelerate the convergence of G. The one-dimensional convolutional layer of each ups-block halves the number of channels until it reaches 1. Then, two dense layers are used to produce the final output, whose dimensions are the same as those of the real data. The structures of D and G are almost symmetrical, except for the subsampling blocks (subs-blocks), as shown in Fig. 4 . Each subs-block involves a one-dimensional convolutional layer, a LeakyReLU layer and a dropout layer. The 1D CNN of each subs-block doubles the number of channels until it reaches 128. The hyperparameter settings for the three types of GANs are based on empirical settings[17]. The optimizer of the G and D for each of the three GANs is ADAM[18], and exponential decay[19] is applied to the learning rate schedule for G and D to determine the optimal learning rate. The 1D convolutional kernels in the 1D CNN are configured with 20 kernels based on the length of the training signals. The output values of G and the input values of D and G are normalized to [-1,1], and the input signals of the three GANs are resampled at a rate of 10 kHz.

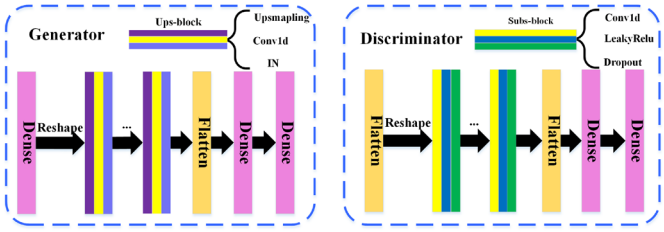

Fig. 4. Network architecture of the proposed GAN-based approach.

D. Data collection

To assess the capability of generative models in capturing and generalizing the distribution of underwater acoustic channel characteristics across various conditions, an sea trial was conducted in the Laoshan Shazikou (LSSZK) area in January 2022. The sea depth was approximately 20 m, the transmitter and the receiving hydrophone were both deployed at a depth of 3 m, and the receiver was a 4-element vertical line array with an interelement spacing of 1 m. The real training received signals were taken from one of the receiving hydrophones. The ocean temperature, salinity and SSP data ssp_{ori} were measured by the transmitting vessel using a conductivity-temperature-depth (CTD) profiler during the experiment. ssp_{ori} is shown in Fig. 5. The center frequency of the continuous-wave (CW) signal transmitted in the experiment was 3 kHz, the pulse width was 0.1 s with a regular interval of 1 s, the number of transmitted signal frames was 400, and the sampling frequency was 48 kHz.

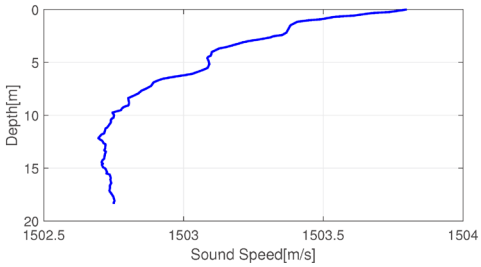

Fig. 5. Experimental measured SSP in LSSZK.

The two ships anchored at a distance of 1.8 km . The current was maintained at a speed of 2 knots, with the transmitting and receiving vessels in motion relative to each other during signal transmission. The experiment spanned a total of 440 seconds, throughout which 400 frames of signal were collected. Correspondingly, we had 400 frames of real UWA CIR and 400 frames of Bellhop simulated CIR. We selected the first 300 frames as the training dataset and the remaining 100 frames as the test dataset. Notably, during these two periods, the distance between the receiving and transmitting ships gradually increased, indicating different motion dynamics. This process was considered a small-scale spatial variation. The generative model was trained on the training dataset to capture the distribution characteristics of the UWA channel dynamic physical processes. Once the model had achieved convergence through training, we deployed the test dataset to assess its performance. The simulation results revealed that the channel characteristics produced by the generator closely matched the distribution of the test real UWA channel characteristics, thereby confirming the generative model's ability to generalize. The determination of the received SNR was based on processing of a series of CW signals. The received energy was acquired by integrating its amplitude, and the integration time corresponded to the duration of a single CW signal. Prior to transmitting the CW signal, a noise signal of the same duration was collected, and its energy was determined through amplitude integration. The energy of the pure signal was approximated by subtracting the noise energy from the received energy. The ratio of the signal energy to the noise energy was expressed in dB to obtain the single reception SNR. The SNR for the LSSZK experiment was calculated to be 31.3 dB. At this SNR, the results obtained through the application of OMP channel estimation represented the true channel. The ray-tracing BELLHOP model is used to generate simulation data $\mathbf{y}_{b,k}$ in our study. In this paper, a weak perturbation is added to the ssp_{ori} of the receiver over a certain period of time to obtain small-scale simulation channel conditions. $\mathbf{y}_{b,k} = \text{BELLHOP}(\mathbf{info}_k) * \mathbf{x}_t$, where BELLHOP$(\cdot)$ operates on the given experimental information $\mathbf{info}_k = \left[\mathbf{ssp}_k^T, \mathbf{env}^T\right]^T$ of the k th frame and out-

puts CIR $\mathbf{h}_{b,k}$ of the k th frame, where $\mathbf{ssp}_k$ is obtained by measured ssp_{ori}. **env** consists of empirical oceanic environmental parameters, the water depth 18.7 m, seabed sound speed 1800 m/s, seabed density 1.8 kg/m^3, seabed attenuation coefficient 0.5 dB/λ, seafloor topography (flat, acoustic half-space), sea surface fluctuations (flat, vacuum-type), source depth 3 m, source angle (-90°, 90°), receiver depth 3 m, and receiving distance 1.8 km.

introducing random variations of (-0.01, 0.01) m/s to the

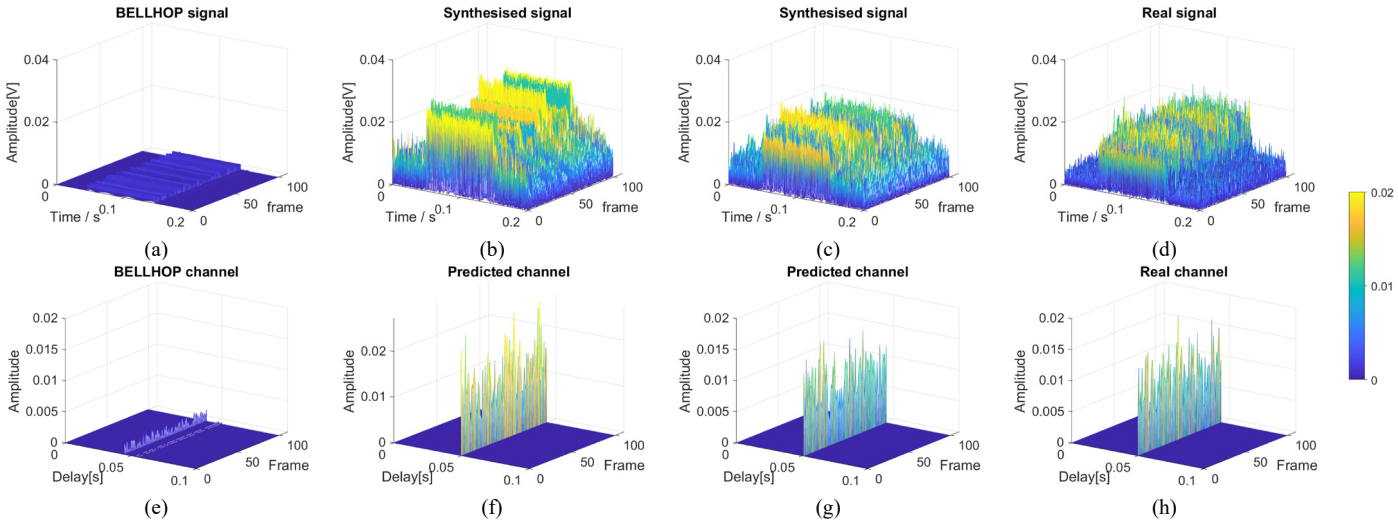

Fig. 6. Qualitative visual signal modeling results of DCWGAN-GP (b), DCWGAN-GP^{B} (c) at iteration 1600 and BELLHOP signals (a) and the real received signals (d) are shown with SNR=10dB. Qualitative visual channel modeling results of DCWGAN-GP (f), DCWGAN-GP^{B} (g) at iteration 1600 and BELLHOP channels (e) and the real channels (h) are shown with SNR=10dB.

IV. EXPERIMENTAL RESULTS

A. Evaluation Metrics

The MAE is used in our study. The MAE is a widely utilized metric for assessing model performance, it quantifies the average absolute error between the samples generated by the tested model and the actual samples. The MAE_{sig} and MAE_h of the k th frame can be expressed as follows:

$$\mathrm{MAE}_{sig} = \frac{1}{N}\sum_{i=1}^{N}\left|\mathbf{y}_{r,k}(i) - \hat{\mathbf{y}}_{g,k}(i)\right| \tag{10}$$

$$\mathrm{MAE}_{h} = \frac{1}{P}\sum_{i=1}^{P}\left|\mathbf{h}_{r,k}(i) - \hat{\mathbf{h}}_{g,k}(i)\right| \tag{11}$$

where $\mathbf{y}_{r,k}(i)$ and $\hat{\mathbf{y}}_{g,k}(i)$ represent the true signal and synthesized signal of the k th frame, respectively; $\mathbf{h}_{r,k}(i)$ and $\hat{\mathbf{h}}_{g,k}(i)$ denote the corresponding channel estimation results, i represents sample point.

B. Performance Analysis

During the generation stage, 100 frames of signals are generated using the test information $\mathbf{info}_{\mathrm{k}}$ and transmitted signal $\mathbf{x}_t$. A quantitative comparison is conducted between the generated signals, the BELLHOP signals, and the real signals. The results are shown in TABLE I. the mean and variance of the MAE_{sig}^{B} values for the 100 frames of DCWGAN-GP^{B} are the lowest at 0.0033 and 8.41e-7, respectively, improving the results of the BELLHOP signal modeling approach. DCWGAN-GP^{B} captures most of the energy inherent in the real signals and exhibits more robust modeling performance than DCWGAN, DCWAN^{B}, DCGAN, and DCGAN^{B}. From a quantitative perspective, the modified DCWGAN-GP^{B} effectively refines the BELLHOP signal modeling results.

TABLE I. MAE_h AND MAE_{sig} PERFORMANCE COMPARISON AMONG VARIOUS GANS WITH AN SNR OF 10 dB.

Models	**mean of** MAE_{sig}	**variance of** MAE_{sig}	**mean of** MAE_h	**variance of** MAE_h
DCWGAN-GP^{B}	**0.0033**	**8.41e-7**	**0.0038**	**7.66e-6**
DCWGAN-GP	0.0049	3.36e-6	0.0059	1.76e-5
DCWGAN^{B}	0.0040	1.69e-6	0.0045	1.33e-5
DCWGAN	0.0048	1.30e-6	0.0052	1.29e-5
DCGAN^{B}	0.0033	1.97e-6	0.0044	1.24e-5
DCGAN	0.0042	1.17e-6	0.0053	1.27e-5
BELLHOP	0.0047	1.87e-6	0.0089	1.35e-5

Fig. 6(a) and Fig. 6(d) show that due to the limited availability of ocean environmental parameters, there is a significant difference in amplitude between BELLHOP signals and real signals, former has a smaller amplitude. From Fig. 6(b) and Fig. 6(c), it can be seen that the signal modeling results of DCWGAN-GP are not ideal in finite iterations, and the diversity of the generated signals is poor. However, after mapping by the generator of DCWGAN-GP^{B}, the generated signals are qualitatively visual similar to the real signals in terms of amplitude and diversity.

We now analyze the channel modeling results obtained by employing the OMP algorithm. The amplitude distribution of the direct path is worthy of attention. The JSD between the direct path distributions of the proposed modeling methods and the true direct path distribution is computed

using JSD. The smaller the JSD is, the closer the distributions are to each other. The JSD results are shown in TABLE II. The JSD of the proposed modeling method (DCWGAN-GP^{B}) is the smallest among those of the six methods. TABLE I. reveals that DCWGAN-GP^{B} exhibits the lowest mean and variance for MAE_h^B, with values of 0.0038 and 7.66e-6, respectively, resulting in a significant 57.3 % improvement over the MAE_h obtained from the channel modeling approach without BELLHOP.

From Fig. 6(e) and Fig. 6(h), it is apparent that the amplitude difference between the BELLHOP modeling channels and the real channels is significant due to the limited availability of ocean environmental parameters. The real channels represent single path, commonly known as the direct path, while the BELLHOP channels consist of multiple paths, known as multi-path. From a visual perspective, Fig. 6(g) and Fig. 6(f) shows that DCWGAN-GP^{B} can effectively model real channels in terms of channel delay and amplitude, while the channel amplitude modeled by DCWGAN-GP is relatively higher due to its higher signal energy during the signal modeling phase.

TABLE II. THE JSD BETWEEN REAL DIRECT PATH DISTRIBUTION AND THE DIRECT PATH DISTRIBUTION MODELED BY EACH ALGORITHM UNDER AN SNR OF 10 dB.

Models	JSD	Models	JSD
DCWGAN-GP^{B}	**0.0057**	DCWGAN	0.1108
DCWGAN-GP	0.0136	DCGAN^{B}	0.0911
DCWGAN^{B}	0.0299	DCGAN	0.0356

V. CONCLUSION

In this paper, a generative model-based method for modeling UWA channels under conditions with partial master oceanic environmental parameters is developed. Compared to vanilla GANs, the incorporation of the outputs of BELLHOP into the frameworks of generative models as priors significantly improves their training speed and stability. Moreover, this method mitigates the approximations and unrealistic assumptions made by BELLHOP by providing real field experimental signals to the generative models. The generative models effectively capture the statistical characteristics of real received UWA signals. Well trained GANs are able to generate CIRs that resemble real CIRs and possess the ability to generalize to small-scale temporal variations. We conducted a comparative analysis among three different types of generative models that incorporated the outputs of BELLHOP. The results of field experiments conducted in shallow water showed that, compared with the traditional ray-tracing channel model (BELLHOP), DCWGAN-GP^{B} achieved significantly modeling performance.

ACKNOWLEDGMENT

This research was supported by the National Natural Science Foundation of China (grant no. 62201166).

REFERENCES

[1] M. Stojanovic, "Underwater Acoustic Communications: Design Considerations on the Physical Layer," in *2008 Fifth Annual Conference on Wireless on Demand Network Systems and Services*, Garmisch-Partenkirchen, Germany: IEEE, Jan. 2008, pp. 1–10.

[2] M. Stojanovic and J. Preisig, "Underwater acoustic communication channels: Propagation models and statistical characterization," *IEEE Commun. Mag.*, vol. 47, no. 1, pp. 84–89, Jan. 2009.

[3] P. Qarabaqi and M. Stojanovic, "Statistical Characterization and Computationally Efficient Modeling of a Class of Underwater Acoustic Communication Channels," *IEEE J. Ocean. Eng.*, vol. 38, no. 4, pp. 701–717, Oct. 2013.

[4] B. Tomasi, G. Zappa, K. McCoy, P. Casari, and M. Zorzi, "Experimental study of the space-time properties of acoustic channels for underwater communications," in *OCEANS'10 IEEE SYDNEY*, May 2010, pp. 1–9.

[5] H. Ghannadrezaii and J.-F. Bousquet, "Demonstration of Underwater Channel State Information Acquisition in Grand Passage, Nova Scotia," *IEEE Journal of Oceanic Engineering (2023).*

[6] P. C. Etter, *Underwater acoustic modeling and simulation*, Fifth edition. Boca Raton: CRC Press, Taylor & Francis Group, 2018.

[7] A. Zielinski, Y.-H. Yoon, and L. Wu, "Performance analysis of digital acoustic communication in a shallow water channel," *IEEE J. Ocean. Eng.*, vol. 20, no. 4, pp. 293–299, Oct. 1995.

[8] Xueyi Geng and Adam Zielinski, "An eigenpath underwater acoustic communication channel model," in *"Challenges of Our Changing Global Environment". Conference Proceedings. OCEANS '95 MTS/IEEE*, San Diego, CA, USA: IEEE, 1995, pp. 1189–1196.

[9] M. Chitre, "A high-frequency warm shallow water acoustic communications channel model and measurements," *J. Acoust. Soc. Am.*, vol. 122, no. 5, pp. 2580–2586, Nov. 2007.

[10] D. Middleton, "Channel Modeling and Threshold Signal Processing in Underwater Acoustics: An Analytical Overview," *IEEE J. Ocean. Eng.*, vol. 12, no. 1, pp. 4–28, Jan. 1987.

[11] R. Otnes, P. A. van Walree, and T. Jenserud, "Validation of Replay-Based Underwater Acoustic Communication Channel Simulation," *IEEE J. Ocean. Eng.*, vol. 38, no. 4, pp. 689–700, Oct. 2013.

[12] A. Creswell, T. White, V. Dumoulin, K. Arulkumaran, B. Sengupta, and A. A. Bharath, "Generative Adversarial Networks: An Overview," *IEEE Signal Process. Mag.*, vol. 35, no. 1, pp. 53–65, Jan. 2018.

[13] M. Heusel, H. Ramsauer, T. Unterthiner, B. Nessler, and S. Hochreiter, "GANs Trained by a Two Time-Scale Update Rule Converge to a Local Nash Equilibrium," in *Advances in Neural Information Processing Systems*, Curran Associates, Inc., 2017.

[14] G. Z. Karabulut and A. Yongacoglu, "Sparse channel estimation using orthogonal matching pursuit algorithm," in *IEEE 60th Vehicular Technology Conference, 2004. VTC2004-Fall. 2004*, Sep. 2004, pp. 3880-3884 Vol. 6.

[15] I. Gulrajani, F. Ahmed, M. Arjovsky, V. Dumoulin, and A. Courville, "Improved Training of Wasserstein GANs," in *Advances in Neural Information Processing Systems 30 (nips 2017)*.

[16] K. Hornik, M. Stinchcombe, and H. White, "Multilayer feedforward networks are universal approximators," *Neural Netw.*, vol. 2, no. 5, pp. 359–366, Jan. 1989.

[17] J. Brownlee, *Deep Learning for Time Series Forecasting: Predict the Future with MLPs, CNNs and LSTMs in Python*. Machine Learning Mastery, 2018.

[18] D. P. Kingma and J. Ba, "Adam: A Method for Stochastic Optimization." arXiv, Jan. 29, 2017.

[19] Z. Li and S. Arora, "An Exponential Learning Rate Schedule for Deep Learning." arXiv, Nov. 21, 2019.